Comparison of different olivines for biomass steam gasification

R. Rauch[a], K. Bosch[a], H. Hofbauer[a], D.Świerczyński[b], C.Courson[b], A.Kiennemann[b],
[a] *Vienna, University of Technology; Institute of Chemical Engineering, Getreidemarkt 9/166, A-1060 Vienna, Austria*
[b] *LMSPC-ECPM, UMR 7515 - 25, rue Becquerel - 67087 Strasbourg Cedex 2 – France*

ABSTRACT: Natural olivine (iron and magnesium orthosilicate ((Mg,Fe)2SiO4) has been chosen as bed material for the FICFB gasification process which is an innovative process to produce a high-grade synthesis gas with low nitrogen content and high calorific value from solid fuels. This process is demonstrated at the biomass CHP plant Guessing at a scale of 8MW fuel input.
The choice of olivine is justified by its hardness required for the use in a fluidised bed and its higher catalytic activity in biomass steam gasification compared to silica or dolomite. In this paper a comparison of two different natural iron-bearing olivines is presented.

INTRODUCTION

A dual fluidized bed system allows the treatment of separated gas streams with the same circulating solid. Various applications using dual fluidized bed systems such as adsorption processes and catalytic cracking can be found in literature [1]. At Vienna University of Technology a dual fluidized bed system for steam gasification was developed jointly by the Institute of Chemical Engineering and Repotec and is currently demonstrated at a scale of $8MW_{fuelinput}$ at the biomass CHP in Guessing, Austria [2]. This gasification concept allows to produce a high grade product gas (LHV 10 - 14 MJ/m³). Gasification reactions take place in a bubbling fluidized bed. Remaining char is carried with the circulating bed-material into the combustion zone. Char and additional fuel for temperature control is burned in the combustion zone operating at turbulent flow-regime. The heated bed-material is separated from the gas in a cyclone and transferred back to the gasification zone. This concept is illustrated in Fig. 1. The hot bed-material supplies the endothermic gasification reactions with heat. The solid

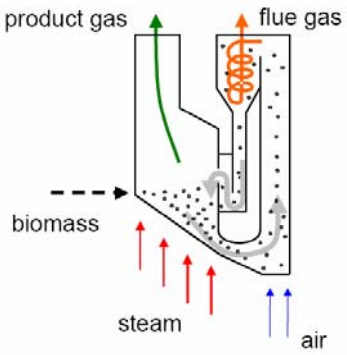

Fig. 1: principle of FICFB-gasification process

circulation between gasification and combustion zone is necessary for heat supply of gasification reactions. The higher the solid circulation rate, the lower the temperature difference between gasification and combustion zone. Moreover, higher solid flux between the fluidized beds conveys more char from the gasification to the combustion zone, which reduces the required amount of additional fuel.

The FICFB-gasification system has - in contrast to conventional gasifiers operated with air - the advantage that it produces a nitrogen-free gas, which after appropriate cleaning and treatment is besides as source of energy also suitable as synthesis gas in the chemical industry.

One essential parameter for the gasification system is the type of bed material, which is used. For fluidised bed gasifiers different bed materials are described in literature. Silica sand is often used as bed material, but it has no catalytic activity. Dolomite, calcite and magnesite are the most investigated bed materials in relation to their catalytic activity in tar destruction [3,4,5]. Also chemical compounds of iron, nickel and other metallic elements were studied to obtain their potential on tar reduction [6,7]. In the FICFB-gasification system the bed material was selected by applying the following criteria:

(1) attrition resistance
(2) catalytic activity in hydrocarbon and tar reforming
(3) transport of oxygen from combustion to gasification zone

In previous work [8,9] different bed materials were investigated and olivine (iron and magnesium orthosilicate) was selected as bed material for the demonstration plant because of its attrition resistance and its catalytic activity. Two olivines from different sources (olivine A and olivine B) were used in the 8MW demonstration plant in Guessing to investigate if there is a difference in the catalytic behaviour of the two olivines.
The aim of this paper is a comparison of the results obtained with the two olivines, an explanation of the observed difference, and a proposal for solutions to increase the activity of olivines for tar reforming.

CHARACTERISATION OF OLIVINE A AND B

CHARACTERIZATION METHODS

The crystalline phases contained in the samples were examined by powder X-ray diffraction (XRD) on a Siemens D500TT diffractometer using Cu Kα radiation,
To quantify the amount of reducible iron, the reducibility of the olivines has been determined by temperature programmed reduction (TPR) performed on 200 mg of catalyst placed in a U-shaped quartz tube (6.6mm ID). The reductive gas mixture ($H_2 = 0.12$ L.h^{-1} and $Ar = 3$ L.h^{-1}) passed through the reactor heated from room temperature to 950°C with a slope of 15°C.min^{-1} then maintained at 950°C until the end of H_2 consumption showed by the baseline return. A thermal conductivity detector (TCD) was used for quantitative determination of hydrogen consumption.
The ^{57}Fe Mössbauer spectra were recorded at liquid nitrogen temperature with ^{57}Co source dispersed in rhodium matrix. From the obtained spectra, the isomeric shifts were

determined in comparison with metallic iron standard at room temperature. To identify the different forms of iron present in the sample, the spectra were fitted with MossFit computer program.

CHEMICAL COMPOSITION

The chemical composition of the two olivines is given in Table 1. Both olivines have similar composition. The only main difference that could be noticed is the iron content which is slightly lower in olivine B. Both olivines contain also small amounts of other elements (Ni, Al, Cr, Ca, Mn).

Table 1: chemical composition of olivines (main components)

	MgO	SiO_2	Fe_2O_3	NiO
olivine A	48-50	39-42	8-10.5	0.5
olivine B	48.5-50	41.5-42.5	6.8-7.3	0.3-0.35

Table 2: chemical composition of olivines (minor components)

	Al_2O_3	Cr_2O_3	CaO	MnO
olivine A	< 0.6	< 0.6	< 0.2	0.06
olivine B	0.4-0.5	0.2-0.3	0.05-0.1	0.05-0.1

X-RAY DIFFRACTION (XRD)

XRD patterns of olivines calcined at temperatures ranging from 900 to 1400°C are shown in Fig. 2.

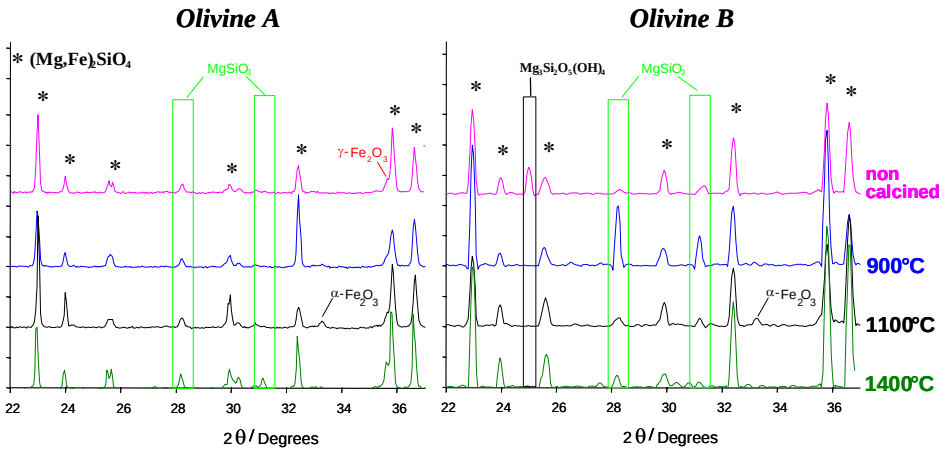

Fig. 2: XRD patterns of olivines A and B calcined at different temperatures.

XRD of olivine A without pre-treatment shows that the main lines are close to those of the Mg_2SiO_4 forsterite (34-0189 JCPDS file). The secondary crystalline phases observed are the $MgSiO_3$ phase - enstatite (19-0606 JCPDS file) visualised by its

100-intensity line at 28.2 (2θ) and iron oxides: α–Fe_2O_3 and γ–Fe_2O_3. Similar diffraction patterns are obtained for sample calcined at 900°C. From 900 to 1100°C an increase of intensity of the main α–Fe_2O_3 line can be observed with a maximum at 1100°C. After calcination at 1400°C, the intensities of the strongest lines of the secondary phases $MgSiO_3$ and γ–Fe_2O_3 increase and the strongest α–Fe_2O_3 line decrease significantly.
For olivine B the main crystalline phase (forsterite) is similar to that of olivine A in all non calcined and calcined samples. The main difference between the two olivines is the secondary phase composition. In the sample of non calcined olivine B two other silicate phases are present: enstatite $MgSiO_3$, like for olivine A, and serpentine $Mg_3Si_2O_5(OH)_4$. However, no iron oxide can be detected. After calcination at 900°C serpentine phase diseapears and two intense lines of proto-enstatite phase appear in place of enstatite (diffraction lines at the same positions but with different relative intensity). At higher temperatures of calcination intensity of the main lines of $MgSiO_3$ phase decreases to become similar like in the non calcined sample. Iron oxide can be detected only after calcination at 1100°C by the presence of a small peak at ~ 33 (2θ) - main diffraction line of α–Fe_2O_3.

TEMPERATURE PROGRAMMED REDUCTION (TPR)

TPR was performed for olivines without pre-treatment and for olivines calcined at temperature range from 900 to 1400°C.

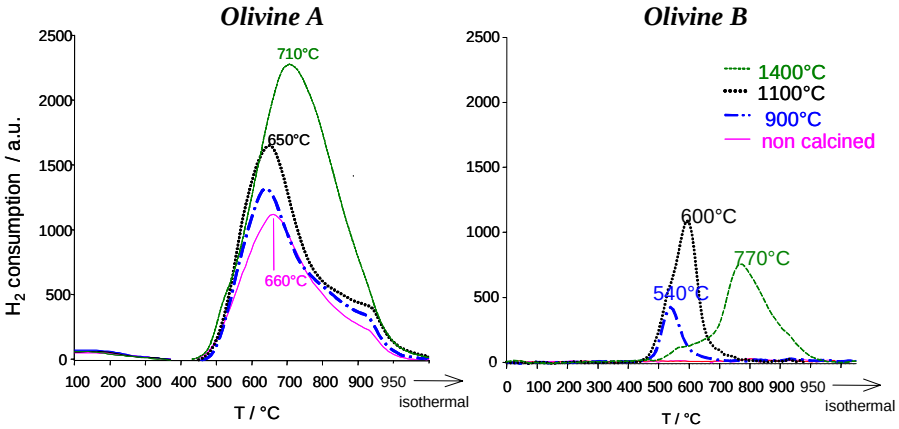

Fig. 3: TPR for olivines A and B calcined at different temperatures.

Reduction profiles for the samples of olivine A calcined at different temperatures are similar and only one reduction peak with maximum between 650 and 710°C depending on the calcinations temperature can be seen. This broad peak is attributed to the reduction of the free iron oxides (α and γ) associated to the olivine structure. The intensity and the width of the reduction peak increases with the temperature of calcination indicating that free iron oxide content increases with calcination temperature as observed by XRD.
Different reducibility is shown in case of olivine B. Non-calcined Olivine B is not reducible which indicates that there is no free iron oxide outside the olivine structure.

TPR profile of sample calcined at 900°C shows a small reduction peak at 540°C. The reduction peak increases with calcination temperature indicating that iron leaves olivine structure to form iron oxide. The amount of free iron oxide depends on the calcination temperature. Also a shift to higher reduction temperatures can be observed with the increase of calcination temperature: reduction at 600°C after calcination at 1100°C and at 770°C for the sample calcined at 1400°C. The shift to higher reduction temperatures could be attributed to the phase transition from α–Fe_2O_3 to γ–Fe_2O_3.
These results show that calcination at higher temperatures leads to iron extraction from the structure of olivines – oxidation of iron II from the olivine structure to iron III in the form of oxide [10]. However, for olivine B the quantity of extracted iron is much lower than for olivine A.
A comparison of the amount of reduced iron dependent on calcination time and temperature for the two olivines is shown in Fig. 4. Using these graphs one can estimate the time and temperature needed for extraction of the desired quantity of iron from the olivine structure. For olivine B a temperature higher than 1400°C (4h calcination) would be required to obtain the same amount of reducible iron as for non treated olivine A. It should be noted that due to high activation energies for diffusion of ions in silicates the diffusivity is rising rapidly with temperature. Generally the increase of the temperature of 100°C causes an increase of diffusion coefficient about 10 times. For olivine B rising the temperature of 100°C (from 900 to 1000°C) permits to decrease the calcination time essentially (about 7 times) in order to obtain the same amount of reducible iron (Fig. 4).

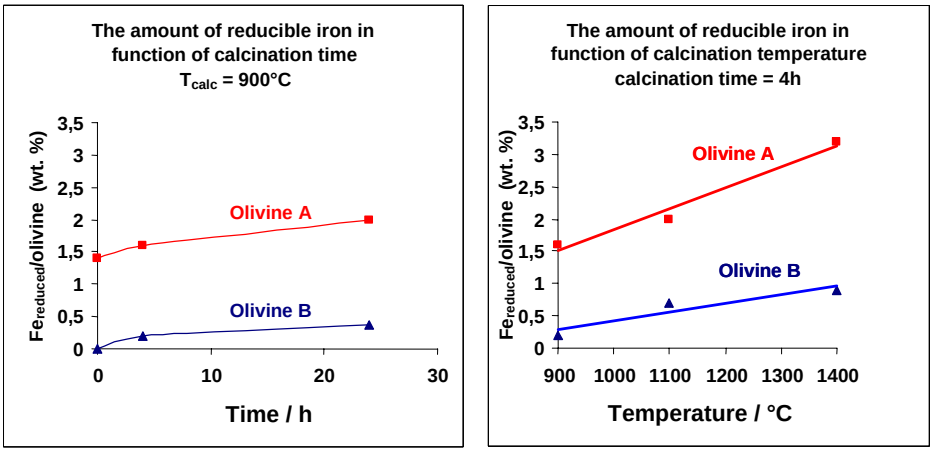

Fig. 4: The amount of reducible iron in olivine dependent time and calcination temperature.

MÖSSBAUER SPECTROSCOPY

In order to quantify the amount of Fe present in different phases the samples were studied by ^{57}Fe Mössbauer spectroscopy. This technique allows calculating the percentage of iron oxidised during calcination. The distribution of iron in different phases obtained by ^{57}Fe Mössbauer spectroscopy is shown in Table 3.

It can be seen that for the non-calcined olivine A already nearly half of the iron is present in form of oxides α and γ. After calcination at 1100°C the amount of iron in the

olivine structure diminishes, due to oxidation of Fe^{2+} to Fe^{3+} , and the amount of α and γ oxides increases. For the non-calcined olivine B all iron is located in the olivine structure. In the sample of olivine B calcined at 1100°C part of iron from the structure of olivine is oxidised to α and γ oxides like in the case of olivine A.

Table 3: Distribution of iron in different phases obtained by 57Fe Mössbauer spectroscopy

Phase	% mol. Fe / Fe total			
	Olivine A		***Olivine B***	
	non calcined	*calc. 1100°C*	*non calcined*	*calc. 1100°C*
$(Mg,Fe)_2SiO_4$	*55*	*17*	*100*	*35*
γ-Fe_2O_3	*14*	*29*	*0*	*24*
α-Fe_2O_3	*31*	*34*	*0*	*41*

Summing up the comparative characterisation of both olivines we can state that although their general composition and phase structure are the very similar the main difference is the integration of iron into the structure of olivine. For olivine A iron is shared between the olivine structure (55%) and iron oxide phase (45%) while in case of olivine B all iron is integrated into the olivine structure. Calcination of iron-bearing olivines in air leads to the oxidation of iron and formation of iron oxides. The amount of iron oxide formed is dependent on calcination time and temperature.

RESULTS FROM BIOMASS CHP GUESSING

The FICFB-gasification process is demonstrated in Guessing, AT. The combined heat and power (CHP) plant has a fuel capacity of 8 MW and an electrical output of about 2 MW with an electrical efficiency of about 25 %. Wood chips with a water content of 20 - 30 % are used as fuel. The plant consists of a dual fluidized bed steam gasifier, a two stage gas cleaning system, a gas engine with an electricity generator, and a heat utilization system. A flow chart of the biomass CHP is given in Fig. 5.

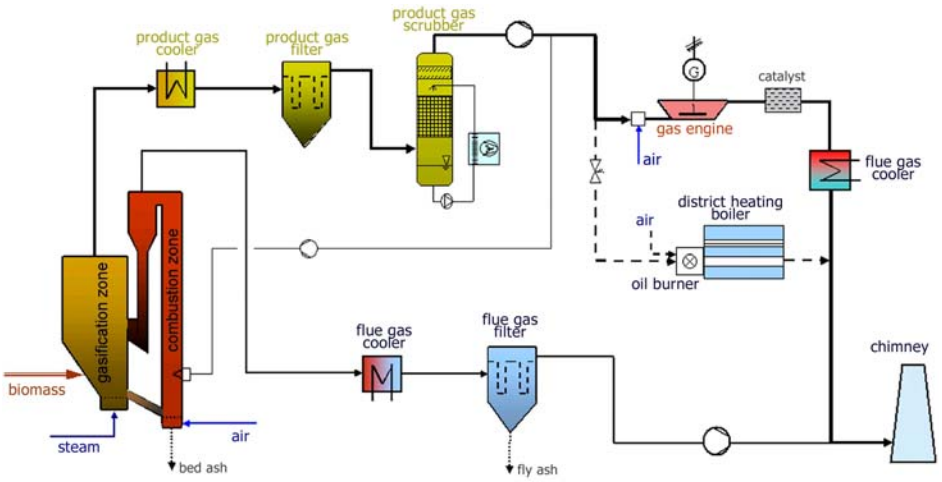

Fig. 5 : Flow chart of biomass CHP Guessing

The producer gas is cooled and cleaned by a two stage cleaning system . A water cooled heat exchanger reduces the temperature from 850 – 900°C to about 150 - 180°C. The first stage of the cleaning system is a fabric filter to separate the particles and some of the tar from the producer gas. These particles are returned back into combustion zone of the gasifier. In a second stage the gas is liberated from tar by a scrubber.
Spent scrubber liquid saturated with tar and condensate is vaporized and introduced into the combustion zone of the gasifier. In addition to gas cleaning the scrubber is also used to reduce the temperature of the clean producer gas to about 40 °C which is necessary for the gas engine. The clean gas is finally fed into a gas engine to produce electricity and heat. The flue gas of the gas engine is catalytically oxidised to reduce the CO emissions. The heat of the engine's flue gas is used to product district heat.
The sensible heat of the flue gas for the combustion zone is used for preheating of the air, superheating the steam and also to deliver heat to the district heating system. A gas filter separates the particles before the flue gas is released via a stack to the environment.
The start up of the plant was in January 2002 and until March 2004 9000 hours of operation with the gasifier and the gas cleaning system and 6400 hours of operation with the gas engine could be reached. The overall performance of the CHP plant is very good; however, some minor problems had to be solved. The most important parts operate quite well only the biomass feeding system and the cooler of the producer gas had to be improved.
As bed material for the biomass CHP in Guessing normally olivine A is used. In the period from April 2003 to September 2003.olivine B was used as bed material as olivine A was not available during this period.

RESULTS WITH OLIVINE A

With olivine A the gasifier including the gas cleaning system was operated more than 8000 hours. It can be stated, that with this bed material a continuous operation was successfully demonstrated. A typical gas composition at a gasification temperature of 900°C is given in Fig. 6.

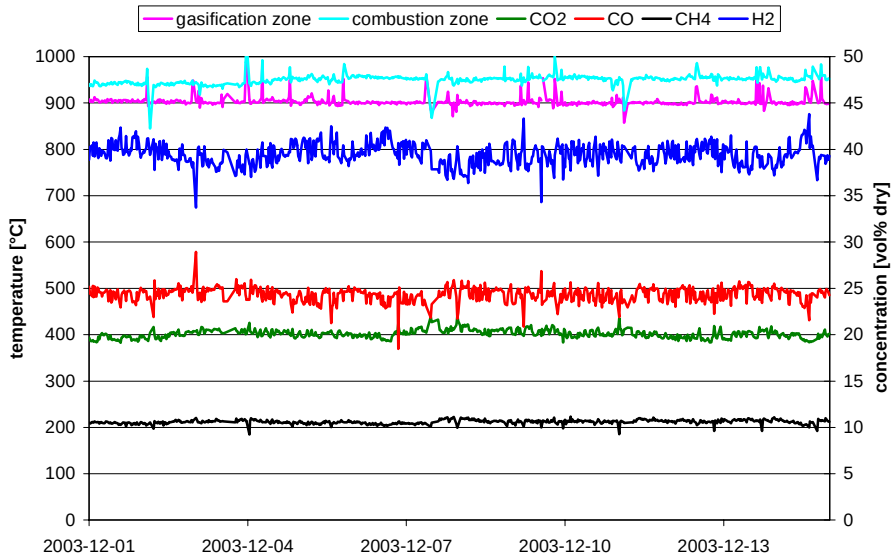

Fig. 6: Gas composition with olivine A

The tar content after the gasifier is typically below 1g/Nm³ and with this low tar content no problems occurs in the gas treatment line. Especially the product gas cooler is very sensitive to the tar content in the product gas. The first 2 days after start up the tar content is higher than in normal operation. This is due to an activation effect of the bed material.

COMPARISON OF OLIVINE A WITH OLIVINE B

Activity in tar reforming

The first tests with olivine B were not successful. The catalytic activity was too low to reduce the tar content in the product gas to a level, that the heat exchanger could be operated successfully. After a period of about 150 hours of operation olivine B had got an activity, that the gasification plant could be operated successfully. The tar content over time of activation (time 0 is the start of the gasifier with new bed material) is shown in Fig. 7.

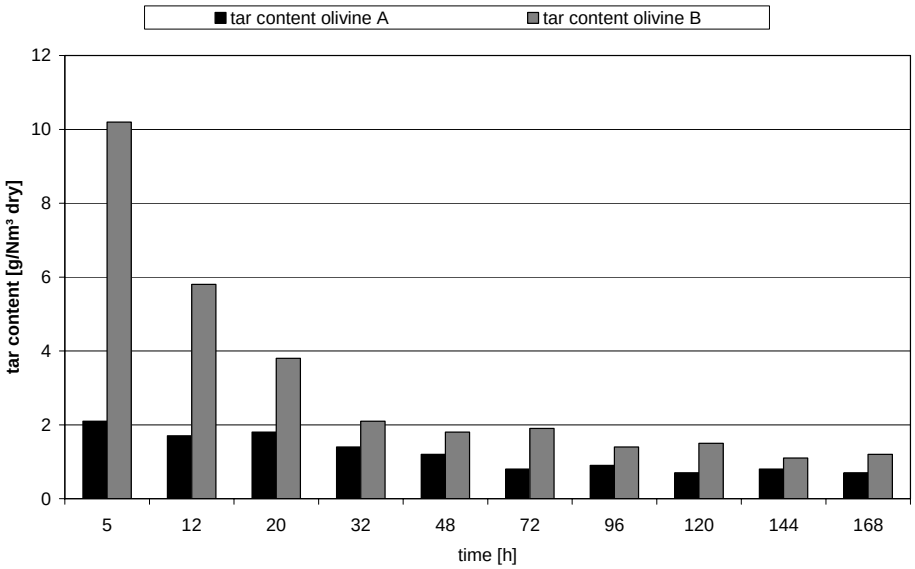

Fig. 7: Comparison of tar content of the olivines

With olivine A the heat transfer is constant from the start up of the plant. This shows that from the beginning of operation the tar content is low enough and no tars deposit inside the heat exchanger. Using non-activated olivine B as bed material the tar content at the beginning is higher and tars deposit inside the heat exchanger.

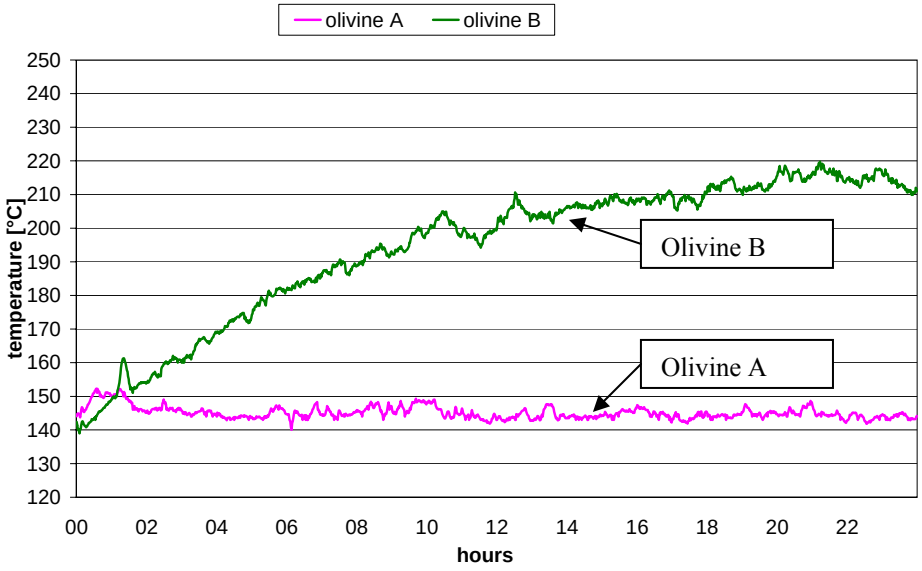

Fig. 8: Comparison of temperatures after product gas heat exchanger

Product gas composition

Also the gas composition changed during the activation of the olivine. The gas composition for olivine A and olivine B for the first run and olivine B when active is shown in Table 4.

Table 4: Comparison of gas composition for olivine A and B

Gas component	Olivine A	Olivine B first run	Olivine B activated
H_2	39.6	34.2	39.9
CO	26.0	29.9	26.6
CO_2	18.7	20.9	19.2
CH_4	11.8	10.6	10.3
C_2H_4	2.0	2.2	2.5

The change of the gas composition can be related mainly to the CO-shift reaction:

$$CO + H_2O \rightarrow CO_2 + H_2$$

As well known from the literature iron species are proposed to be active for this reaction.

After the activation time (about 150 hours of operation) olivine B reacted in the same way as olivine A. Analysis (SEM coupled with X-ray microanalysis) of both olivines after gasification tests showed the presence of about 10-20% of additional Ca on the surface of olivines. It is possible that calcium containing phase plays also a role in reduction of tars.

CONCLUSION

Olivine A is immediately catalytically active. This results in a tar-content in the raw product gas of 2 g/Nm³dry at the start and the tar is reduced to below 1g/Nm^3 after 48 hours of operation. Olivine B needs about one week of operation to reach a similar catalytic activity as olivine A. The tar content in the product gas by using olivine B goes down from more than 10 g/Nm³dry at the beginning to about 1.5 g/Nm³dry after one week of operation.
Characterisation of the olivines versus calcination temperature by TPR, XRD and Mössbauer spectroscopy have revealed the presence of iron oxides outside of olivine structure ($(Mg,Fe)_2SiO_4$) in the olivine A. In case of olivine B, no free iron oxide was observed. The quantity of iron oxide can be increased by calcination of olivine in air which causes oxidation of Fe^{2+} from the olivine structure to Fe^{3+} in the form of α and γ oxides. Taking into account the results of gasification tests and characterisation of the olivines we can consider a hypothesis that the presence of iron oxides outside of olivine structure plays an important role in the olivine activity. However, considering the results of characterisation after operation, showing the presence of Ca on the olivines

surface, the influence of Ca containing phase on the activity can not be excluded and has to be investigated further.

Olivine has proven its suitability in biomass gasification in a dual fluidised bed reactor. It combines on the one hand the attrition resistance as bed material for fluidised beds and on the other hand the catalytic activity for tar reforming. It ensures in a single step process both biomass gasification and reforming of unwanted hydrocarbons (especially tar) to obtain a high grade hydrogen rich gas for various applications (e.g. electricity production, synthesis gas).

ACKNOWLEDGEMENT

This work has been performed partly under the EC, Project No. ENK5-CT2000-00314 and partly under the Austrian funds program K_{net}. The financial support of the European Community, of the Ministry of Economy and Labour of Austria, and of the Federal States of Niederoesterreich and Burgenland is gratefully acknowledged.

REFERENCES

1 Hofbauer H. (1995) Internally Circulating Fluidized Beds, Fundamental and Applications, Proc. of the 1st SCEJ Symposion on Fluidization, Tokyo.

2 Hofbauer, H. et al. (2002) Six Years Experience with the FICFB-Gasification process, 12th European Conference and Technology Exhibition on Biomass for Energy, Industry and Climate Protection, Amsterdam.

3 Corella, J., Aznar, M.-P., Gil, J. and Caballero, M. A. (1999) Biomass gasification in fluidized bed: where to locate the dolomite to improve gasification?, Energy & Fuels pp 1122-1127.

4 Delgado, J., Aznar, M. P. and Corella, J. (1996) Calcined Dolomite, Magnesite, and Calcite for Cleaning Hot Gas from a Fluidized Bed Biomass Gasifier with Steam: Life and Usefulness, Ind. Eng. Chem. Res. pp 3637-3643.

5 Garcia, X. A., Alarcon, N. A. and Gordon, A. L. (1999) Steam gasification of tars using a CaO catalyst, Fuel Processing Technology, pp 83-102.

6 Albrecht, J., Greil, C., Bareuther, E. and Sturm P. (2000) Fluidized-bed air oxidation for removal of heavy volatile aromatic hydrocarbons derived from gasification of biomass and wastewater treatment sludge, Deutschland: Metallgesellschaft AG, 60325 Frankfurt, DE.

7 Ising M. (2002) Zur katalyschen Spaltung teerartiger Kohlenwasserstoffe bei der Wirbelschichtvergasung von Biomasse“, PhD-Thesis, Fraunhofer-Institut für Umwelt-, Sicherheits- und Energietechnik UMSICHT, Oberhausen.

8 Rapagnà S., Jand N., Kiennemann A., Foscolo P.U. (2000) Steam-gasification of biomass in a fluidised-bed of olivine particles, Biomass & Bioenergy, 19 pp 187.

9 Veronik G. (1997) Vergasung von Biomasse in intern zirkulierenden Turbowirbelschichtsystemen, PhD-Thesis, University of Technology, Vienna.

10 Champness P.E. (1970) Mineralogical magazine, 37 / 291 pp 790.